THE JOURNAL OF BIOLOGICAL CHEMISTRY VOL. 289, NO. 43, pp. 29751–29765, October 24, 2014

Fibroblast Growth Factor 21 Is Regulated by the IRE1α-XBP1 Branch of the Unfolded Protein Response and Counteracts Endoplasmic Reticulum Stress-induced Hepatic Steatosis*◆

Received for publication, March 15, 2014, and in revised form, August 2, 2014 Published, JBC Papers in Press, August 28, 2014, DOI 10.1074/jbc.M114.565960

Shan Jiang[‡1], Cheng Yan[§1], Qi-chen Fang[‡], Meng-le Shao[§], Yong-liang Zhang[§], Yang Liu[§], Yi-ping Deng[§], Bo Shan[§], Jing-qi Liu[§], Hua-ting Li[‡], Liu Yang[§], Jian Zhou[¶], Zhi Dai[¶], Yong Liu[§2], and Wei-ping Jia[‡3]

From the [‡]Shanghai Key Laboratory of Diabetes Mellitus, Department of Endocrinology and Metabolism, Shanghai Diabetes Institute, Shanghai Clinical Center for Diabetes, and Shanghai Key Clinical Center for Metabolic Disease, Shanghai JiaoTong University Affiliated Sixth People's Hospital, Shanghai 200233, the [§]Key Laboratory of Nutrition and Metabolism, Institute for Nutritional Sciences, Shanghai Institutes for Biological Sciences, Chinese Academy of Sciences, University of the Chinese Academy of Sciences, Shanghai 200031, and the [¶]Department of Liver Surgery, Liver Cancer Institute, Zhongshan Hospital, Fudan University, Shanghai 200032, China

Background: Although both are involved in metabolic homeostasis, the interconnection between ER stress and FGF21 remains incompletely understood.
Results: Directly up-regulated by the IRE1α-XBP1 pathway, FGF21 could alleviate ER stress-induced liver steatosis.
Conclusion: FGF21 acts as a metabolic effector of the UPR program, exerting feedback effects upon lipid metabolism.
Significance: These findings reveal a regulatory mechanism linking FGF21 actions to metabolic ER stress.

Endoplasmic reticulum (ER) stress activates the adaptive unfolded protein response (UPR) and represents a critical mechanism that underlies metabolic dysfunctions. Fibroblast growth factor 21 (FGF21), a hormone that is predominantly secreted by the liver, exerts a broad range of effects upon the metabolism of carbohydrates and lipids. Although increased circulating levels of FGF21 have been documented in animal models and human subjects with obesity and nonalcoholic fatty liver disease, the functional interconnections between metabolic ER stress and FGF21 are incompletely understood. Here, we report that increased ER stress along with the simultaneous elevation of FGF21 expression were associated with the occurrence of nonalcoholic fatty liver disease both in diet-induced obese mice and human patients. Intraperitoneal administration of the ER stressor tunicamycin in mice resulted in hepatic steatosis, accompanied by activation of the three canonical UPR branches and increased the expression of FGF21. Furthermore, the IRE1α-XBP1 pathway of the UPR could directly activate the transcriptional expression of *Fgf21*. Administration of recombinant FGF21 in mice alleviated tunicamycin-induced liver steatosis, in parallel with reduced eIF2α-ATF4-CHOP signaling. Taken together, these results suggest that FGF21 is an integral physiological component of the cellular UPR program, which exerts beneficial feedback effects upon lipid metabolism through counteracting ER stress.

In eukaryotes, the endoplasmic reticulum (ER)[4] is the major site of protein folding and maturation as well as lipid biosynthesis. Accumulation of unfolded or misfolded proteins or perturbation of lipid metabolism at the ER causes ER stress, activating the adaptive cellular response termed the unfolded protein response (UPR) (1–3). In mammals, three canonical signaling branches of the UPR act coordinately to relieve ER stress. These include the ER-resident transmembrane protein inositol-requiring enzyme 1 (IRE1), PKR-like endoplasmic reticulum kinase (PERK), and activating transcription factor 6 (ATF6) (1, 2). IRE1 is evolutionarily the most conserved sensor of ER stress, possessing both protein Ser/Thr kinase and endoribonuclease (RNase) activities (2, 4, 5). Under ER stress conditions, IRE1 is activated through trans-autophosphorylation and dimerization/oligomerization (6, 7), catalyzing the removal of a 26-nuceotide intron within the mRNA that encodes the transcription factor X-box-binding protein 1 (XBP1) (8). This nonconventional splicing event generates an active spliced form of XBP1 (XBP1s) to initiate a critical UPR program (8). Upon sensing ER stress, PERK mediates the second UPR branch through phosphorylating the ubiquitous protein translation

* This work was supported by Ministry of Science and Technology 973 Programs 2011CB504001, 2012CB524900, and 2011CB910900, National Natural Science Foundation of China Grants 81170379, 30988002, 31230036, 81021002, and 91213306 (to W. J. and Y. L.), Young Scientists Fund from National Natural Science Foundation Grant 81200292, and Shanghai Rising-Star Program Grant 13QA1402900 (to H. L.).
◆ This article was selected as a Paper of the Week.
[1] Both authors contributed equally to this work.
[2] To whom correspondence may be addressed: Key Laboratory of Nutrition and Metabolism Institute for Nutritional Sciences SIBS, Chinese Academy of Sciences, 294 Tai Yuan Rd., Shanghai 200031, China. Tel.: 86-21-5492-0244; Fax: 86-21-5492-0291; E-mail: liuy@sibs.ac.cn.
[3] To whom correspondence may be addressed: Shanghai Key Laboratory of Diabetes Mellitus, Dept. of Endocrinology and Metabolism, Shanghai Jiao Tong University Affiliated Sixth People's Hospital, 600 Yishan Rd., Shanghai 200233, China. Tel.: 86-21-6436-9181, ext. 8922; Fax: 86-21-6436-8031; E-mail: wpjia@sjtu.edu.cn.

[4] The abbreviations used are: ER, endoplasmic reticulum; UPR, unfolded protein response; FGF21, fibroblast growth factor 21; NAFLD, nonalcoholic fatty liver disease; PERK, PKR-like endoplasmic reticulum kinase; CHOP, C/EBP homologous protein; LFD, low fat diet; HFD, high fat diet; LKO, liver-specific IRE1α knockout; Tm, tunicamycin; PPAR, peroxisome proliferator-activated receptor; ANOVA, analysis of variance; ERSE, ER stress-response element; Luc, luciferase; EGFP, enhanced GFP.

initiation factor eIF2α, thereby inhibiting cellular mRNA translation (1, 2). In addition, PERK phosphorylation of eIF2α leads to simultaneous induction of the transcription factor ATF4 (9), which in turn drives the expression of its target gene, transcription factor C/EBP homologous protein (CHOP) (10, 11). Together with ATF6, these UPR programs function to maintain homeostasis of the ER and play a pivotal part in managing ER stress to allow for cell survival.

Emerging lines of evidence have also implicated the UPR pathways in metabolic homeostasis (3, 12). ER stress represents an important mechanism that underlies metabolic disorders (13–15), including the development of nonalcoholic fatty liver disease (NAFLD), a hallmark of metabolic syndrome and a major health burden in both developed and developing countries (16, 17). A number of clinical studies have shown increased ER stress markers in both liver and adipose tissues from human subjects with obesity and NAFLD (18–21). Studies in animal models with genetic disruption of the IRE1α, eIF2α, or ATF6α pathway (22, 23) indicated that the three UPR branches may act in concert to prevent the development of hepatic steatosis, which is linked to perpetuated expression of CHOP arising from unresolved ER stress. Despite this recent progress, the physiological mechanism by which each individual UPR branch can affect lipid metabolism during hepatic steatosis has yet to be completely delineated.

Fibroblast growth factor 21 (FGF21), an atypical member of the FGF family, functions as a hormone that has a wide range of endocrine, autocrine, and pharmacological actions on carbohydrate and lipid metabolism (24). It has been shown in mouse models that FGF21 is secreted from the liver in response to extended periods of fasting, and its expression is controlled by PPARα, a master regulator of the starvation response (25, 26). In humans, however, FGF21 is merely modestly induced by PPARα agonists or fasting, and circulating levels of FGF21 are not increased during short term fasting or by ketogenic diets (27, 28). Intriguingly, studies using genetic and diet-induced mouse models of obesity have revealed multiple beneficial effects of FGF21 administration upon a number of metabolic parameters (29–32), including decreased hepatic triglycerides. This makes FGF21 an attractive drug candidate for the treatment of metabolic diseases. Paradoxically, increased hepatic FGF21 expression and plasma FGF21 levels have been documented in obese mice (33). Moreover, we and others have shown that circulating FGF21 levels are elevated in human obese subjects and patients with hypertriglyceridemia, type 2 diabetes, or NAFLD (34–40). Notably, elevated serum levels of FGF21 are closely associated with chronic liver injury and hepatic triglycerides (35, 37), and FGF21 may even serve as an independent predictor of NAFLD (38). While the molecular basis of the increased FGF21 levels in association with metabolic disorders remains elusive, it is currently unclear whether important differences in the regulation and function of FGF21 exist between rodents and humans.

It was recently reported that the expression of FGF21 can be induced by ATF4 during amino acid deprivation or ER stress (41–43). To fully understand the potential physiological connection between the metabolic actions of FGF21 and ER stress, we examined the relationship between hepatic FGF21 expression and activation of the UPR branches in association with hepatic steatosis in mice as well as in human subjects. We found that hepatic FGF21 is transcriptionally up-regulated by the IRE1α-XBP1 pathway of the UPR, which can in turn suppress the eIF2α-ATF4-CHOP pathway in hepatocytes, alleviating ER stress-induced hepatic steatosis.

MATERIALS AND METHODS

Animals—Male C57BL/6J mice, purchased from Shanghai Laboratory Animal Co. Ltd., were housed in laboratory cages at a temperature of 23 ± 3 °C with a humidity of 35 ± 5%. Animals were maintained on a 12-h dark/light cycle with free access to a standard chow diet (Shanghai Laboratory Animal Co. Ltd.) and water. For the diet-induced obesity model, mice at 6 weeks of age were fed for 16 weeks a low fat diet (LFD) containing 10% kcal of fat or a high fat diet (HFD) containing 60% kcal of fat (Research Diets Inc.). For the tunicamycin-induced ER stress animal model, mice at 12 weeks of age were injected intraperitoneally with DMSO or tunicamycin (Sigma) at a dose of 1 mg/kg body weight and sacrificed after 24 h of treatment. Mice with liver-specific knock-out of IRE1α (LKO) were bred as described previously (44). For examination of the effect of FGF21 on ER stress, mice at 12 weeks were treated with DMSO or tunicamycin (1 mg/kg body weight), and starting at 6 h before tunicamycin injection, recombinant mouse FGF21 (PeproTech) was administered intraperitoneally at 1 mg/kg body weight for a total of five times every 6 h. Mice were sacrificed at 24 h after tunicamycin treatment. All animals were killed under anesthetic conditions, and livers were snap-frozen in liquid nitrogen immediately after resection before storage at −80 °C. All experimental procedures and protocols were approved by the Institutional Animal Care and Use Committee at the Institute for Nutritional Sciences, Shanghai Institutes for Biological Sciences, Chinese Academy of Sciences.

Measurement of Serum and Secreted FGF21 Concentrations—Serum FGF21 was measured using the ELISA kit (Millipore) according to the manufacturer's instructions. For secreted FGF21, cell culture medium (3 ml) was collected by centrifugation to remove cellular debris. The supernatant was concentrated to 200 μl using an Amicon Ultra-4 centrifugal filter unit (Millipore). FGF21 concentrations were then determined by ELISA.

Measurement of Serum and Liver Triglycerides—Serum levels of triglycerides were determined using the serum triglyceride determination kit (Sigma). To measure hepatic content of triglycerides, 40–50 mg of mouse liver tissue was homogenized in 0.5 ml of PBS, and 0.4 ml of homogenate was aspirated into a new tube before mixing sufficiently with 1.6 ml of $CHCl_3$/CH_3OH (2:1, v/v). After centrifugation at 3,000 rpm for 10 min at room temperature, the lower organic phase was transferred and air-dried overnight in a chemical hood. The residue was resuspended in 800 μl of 1% Triton X-100 in absolute ethanol, and then the concentration of triglycerides was determined using the serum triglyceride determination kit (Sigma).

Human Liver Samples—Human liver samples were collected from patients of benign focal hepatic lesions undergoing liver surgery at the Department of Liver Surgery (Zhongshan Hospital, Fudan University, Shanghai, China) as described previously

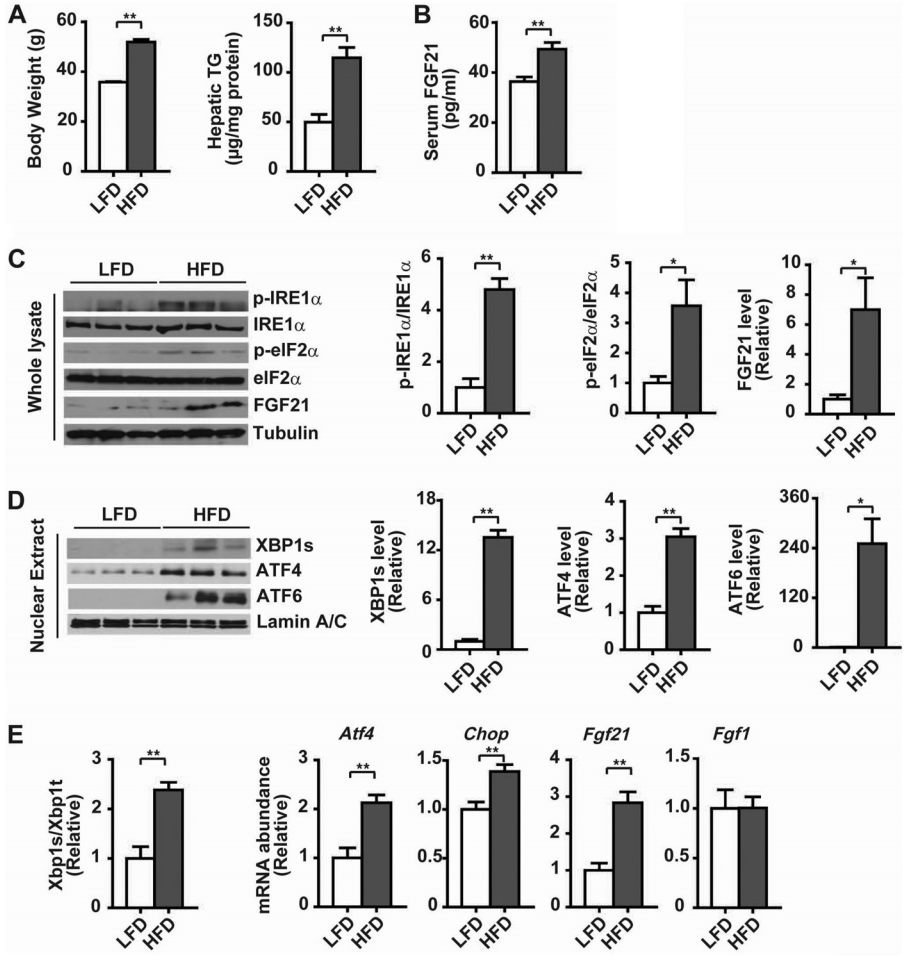

FIGURE 1. **Hepatic UPR activation and FGF21 expression in diet-induced obese mice.** Male C57BL/6 mice at 6 weeks of age were maintained on a LFD (10% fat) or HFD (60% fat) for 16 weeks ($n = 6$ per group). *A,* body weight and hepatic levels of triglycerides (*TG*). *B,* serum levels of FGF21. Data in *A* and *B* are shown as the mean ± S.E. **, $p < 0.01$ by unpaired two-tailed *t* test. *C,* immunoblot analyses of the UPR markers, including phosphorylation of IRE1α (*p-IRE1α*) and eIF2α (*p-eIF2α*), and FGF21 protein abundance in whole liver lysates. Tubulin was used as the loading control, and representative results are shown for three individual mice per group. Ratios of p-IRE1α/IRE1α, p-eIF2α/eIF2α, and FGF21 protein levels were quantified by densitometry from the immunoblots. Relative FGF21 levels were normalized to tubulin. *D,* immunoblot analyses of the abundance of XBP1s, ATF4, and ATF6 proteins in liver nuclear extracts. Lamin A/C was used as the loading control. Relative levels of XBP1s, ATF4 and ATF6 are shown from densitometric quantification of the immunoblots after normalization to lamin A/C. *E,* assessment by quantitative real time RT-PCR of hepatic *Xbp1* mRNA splicing, shown as the ratio of the spliced (*s*) to total (*t*) *Xbp1* mRNA, along with the mRNA abundance of *Atf4*, *Chop*, *Fgf21*, and *Fgf1*. Data in *C–E* are presented as the mean ± S.E. ($n = 6$/group) relative to the LFD-fed control mice. *, $p < 0.05$; **, $p < 0.01$ by *t* test.

(37), including tissues from patients with NAFLD. Diagnosis of NAFLD was according to the guidelines proposed by the Asia-Pacific Working Party (45). Tissues were immediately snap-frozen in liquid nitrogen and stored at −80 °C. All samples had been examined by a pathologist, who was blinded to the study. Hepatic steatosis was classified as grade 0 (1–5%), grade 1 (6–33%), grade 2 (34–66%), and grade 3 (67–100%) (46). Tissue samples used for protein and total RNA preparation were from five patients with severe NAFLD *(i.e.* hepatic steatosis scored as grade 2 or 3) and five controls (*i.e.* hepatic steatosis grade 0), and none of which was pathologically diagnosed as having nonalcoholic steatohepatitis or cirrhosis. The study procedures were approved by the local ethics committee, following the principles of the Declaration of Helsinki. Written voluntary consent was obtained from all subjects before their participation.

Cell Culture and Treatment—Human hepatoma cell line HepG2 was grown in DMEM supplemented with 10% fetal bovine serum, 2 mM glutamine, and antibiotics (100 units/ml penicillin and 100 μg/ml streptomycin) (Invitrogen). For ER stress experiments, cells were incubated in DMEM containing DMSO, 1 μM thapsigargin (Sigma), or 10 μg/ml tunicamycin (Sigma).

Recombinant Adenoviruses—Recombinant adenoviruses for the overexpression of EGFP (control), the wild-type, or the mutant forms of IRE1α were generated as described previously (47). Adenoviruses for XBP1s overexpression and knockdown were the generous gifts from Dr. Ling Qi (Cornell University). The knockdown control adenovirus Ad-sh-LacZ was generated as described with the BLOCK-iT adenoviral RNAi expression system (Invitrogen) in HEK293A cells according to the manufacturer's instructions (48). For infection of mouse primary hepatocytes, viruses were used at a multiplicity of infection of 40, which was measured according to the manufacturer's instructions.

Primary Hepatocytes and Adenoviral Infection—Primary hepatocytes were isolated from male mice at 8–12 weeks of age according to the procedure previously described in detail (48).

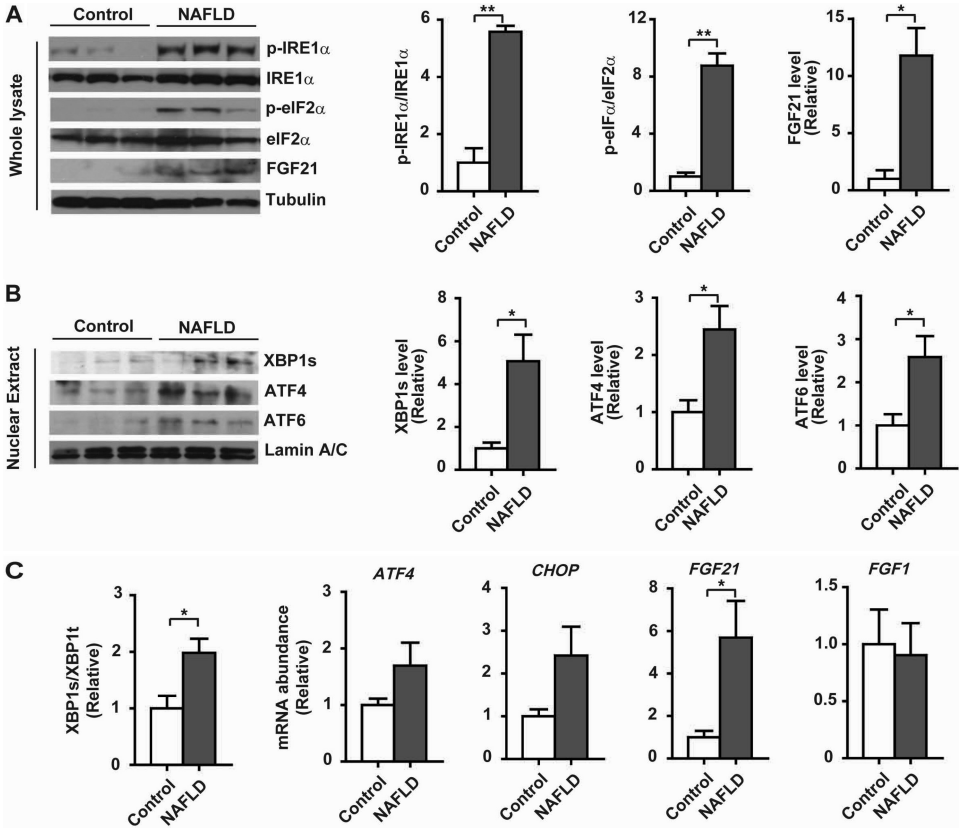

FIGURE 2. **Hepatic UPR activation and FGF21 expression in human NAFLD patients.** Human liver tissue samples were prepared from subjects without or with NAFLD ($n = 5$/group). *A,* immunoblot analyses of the UPR markers p-IRE1α and p-eIF2α and FGF21 protein abundance in whole liver lysates. Tubulin was used as the loading control, and representative results are shown for three individual subjects per group. Ratios of p-IRE1α/IRE1α and p-eIF2α/eIF2α and relative FGF21 levels were quantified. *B,* immunoblot analyses of the abundance of XBP1s, ATF4, and ATF6 proteins in liver nuclear extracts. Lamin A/C was used as the loading control. Results represent three individuals per group. Relative levels of XBP1s, ATF4, and ATF6 were quantified after normalization to lamin A/C. *C,* quantitative RT-PCR analyses of *XBP1* mRNA splicing and the mRNA abundance of the indicated genes. All the results are shown as the mean ± S.E. ($n = 5$/group) relative to the control subjects. *, $p < 0.05$; **, $p < 0.01$ by *t* test.

Briefly, collagenase perfusion was performed through the portal vein of mice after anesthetizing with 50 ml of perfusion buffer. Livers were aseptically removed and cut in a sterile 10-cm cell culture dish with 20 ml of ice-cold perfusion buffer without collagenase. After aspirating with a large-bore pipette, hepatocytes were filtrated through a 70-μm cell strainer (BD Falcon) into a 50-ml centrifuge tube before centrifugation at 50 × *g* for 2 min at 4 °C. Cells were washed with cold hepatocyte wash medium (Invitrogen) three times and resuspended in 15 ml of cold HepatoZYME-SFM medium (Invitrogen) supplemented with 2 mM L-glutamine, 20 units/ml penicillin, and 20 μg/ml streptomycin. After trypan blue staining for determination of viability, cells were plated at 6×10^5 cells/well in 6-well culture dishes or at 3×10^5 cells/well in 12-well dishes pre-coated with collagen. Cells were cultured for at least 8 h before further use. Hepatocytes were infected with adenoviruses for 48 h in the overexpression experiments or for 72 h in the knockdown experiments. Cells were subsequently treated with the desired reagents prior to protein extraction for immunoblotting analysis or total RNA isolation for quantitative real time RT-PCR analysis.

Chemicals, Antibodies, and Immunoblotting—ERK inhibitor U0126 was purchased from Cayman. p-IRE1α antibody was purchased from Novus Biologicals. Antibodies against IRE1α, p-eIF2α, eIF2α, ERK, p-ERK, and lamin A/C were all from Cell Signaling. XBP1s antibody was from BioLegend; α-tubulin antibody was from Sigma; ATF4 antibody was from Santa Cruz Biotechnology; ATF6 antibody was from Imgenex, and FGF21 antibody was from Abcam. For immunoblotting, total proteins were extracted from cells or liver tissues by RIPA buffer (150 mM NaCl, 1% Nonidet P-40, 0.5% sodium deoxycholate, 0.1% SDS, 50 mM Tris-HCl, pH 7.4), and nuclear extracts were prepared using NE-PER nuclear and cytoplasmic extraction kit (Thermo Scientific). Proteins were separated by SDS-PAGE and transferred to polyvinylidene difluoride membrane filters (Millipore). After incubation with the desired antibodies, the blots were developed with SuperSignal West Pico Chemiluminescent substrate (Pierce) or Immobilon Western Chemiluminescent HRP substrate (Millipore).

Quantitative Real Time RT-PCR Analysis—Total RNAs were isolated from cells or liver tissues by TRIzol reagent (Invitrogen), and cDNA was generated by Moloney murine leukemia virus-reverse transcriptase with random hexamer primers (Invitrogen). Real time quantitative PCR was conducted with an ABI Prism 7500 sequence detection system, using the SYBR Green PCR Master Mix (Applied Biosystems). β-Actin was used as an internal control for normalization. The oligonucleotide primers used for each target gene are listed as follows: mouse *ActB*, sense 5′-AGTGTGACGTTGACATCCGTA-3′ and antisense 5′-GCCAGAGCAGTAATCTCCTTCT-3′; mouse *Xbp-1s*, sense 5′-CTGAGTCCGAATCAGGTGCAG-3′ and anti-

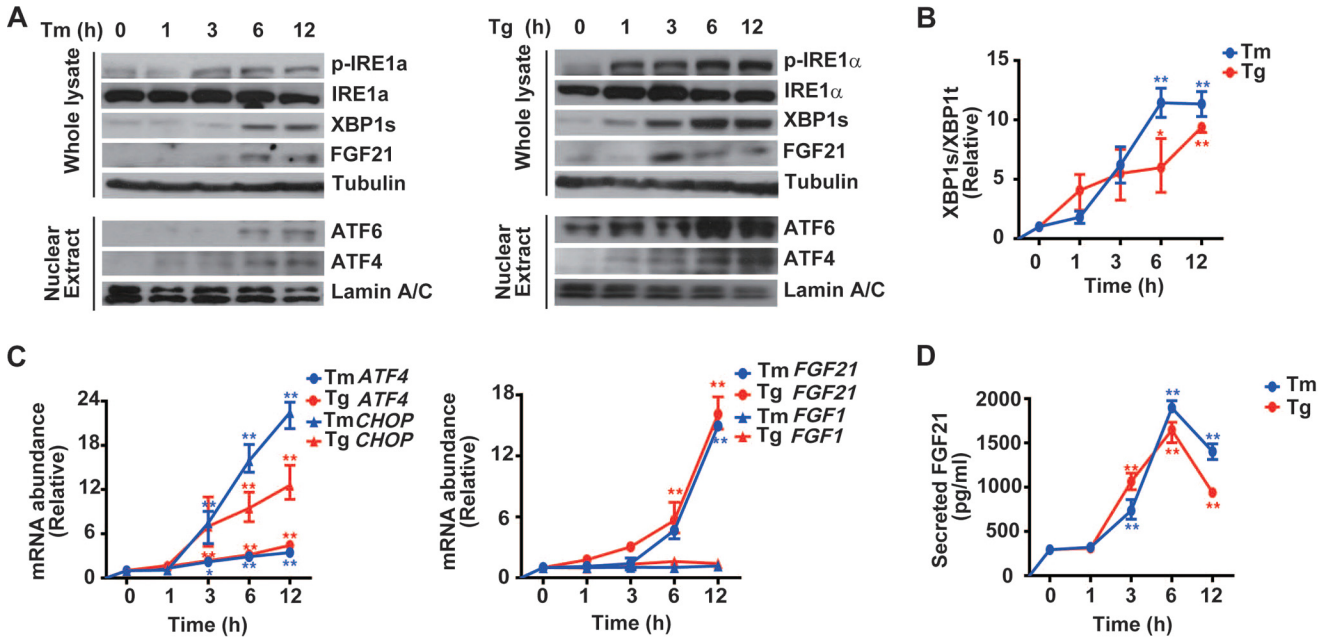

FIGURE 3. **ER stress results in increased expression of FGF21 in HepG2 cells.** HepG2 cells were treated with tunicamycin (*Tm*, 10 μg/ml) or thapsigargin (*Tg*, 1 μM) for the indicated time intervals. *A*, ER stress markers and FGF21 protein abundance were analyzed by immunoblotting from whole cell lysates or nuclear extracts as indicated. Shown are representative results from three independent experiments. *B* and *C*, *Xbp1* mRNA splicing (*B*) and the mRNA abundance of *ATF4*, *CHOP*, *FGF21*, and *FGF1* (*C*) were determined by quantitative RT-PCR. Results were normalized to the values before Tm/thapsigargin treatment and are shown as the mean ± S.E. ($n = 3$ independent experiments). *, $p < 0.05$; **, $p < 0.01$ by one-way ANOVA. *D*, secreted FGF21 levels were measured from the culture medium, shown as the mean ± S.E. ($n = 3$ independent experiments). **, $p < 0.01$ by one-way ANOVA.

sense 5′-GTCCATGGGAAGATGTTCTGG-3′; mouse *Xbp-1t*, sense 5′-TGGCCGGGTCTGCTGAGTCCG-3′ and antisense 5′-GTCCATGGGAAGATGTTCTGG-3′; mouse *Chop*, sense 5′-CTGGAAGCCTGGTATGAGGAT-3′ and antisense 5′-CAGGGTCAAGAGTAGTGAAGGT-3′; mouse *Fgf21*, sense 5′-CTGCTGGGGGTCTACCAAG-3′ and antisense 5′-CTGCGCCTACCACTGTTCC-3′; mouse *Fgf1*, sense 5′-GGGGAGATCACAACCTTCGC-3′ and antisense 5′-GTCCCTTGTCCCATCCACG-3′; human *ACTB*, sense 5′-CATGTACGTTGCTATCCAGGC-3′ and antisense 5′-CTCCTTAATGTCACGCACGAT-3′; human *XBP-1s*, sense 5′-CTGAGTCCGAATCAGGTGCAG-3′ and antisense 5′-ATCCATGGGGAGATGTTCTGG-3′; human *Xbp-1t*, sense 5′-GACGGGACCCCTAAAGTTCTG-3′ and antisense 5′-CTTCTTTCGATCTCTGGCAGTC-3′; human *CHOP*, sense 5′-CAAGAGGTCCTGTCTTCAGATGA-3′ and antisense 5′-TCTGTTTCCGTTTCCTGGTTC-3′; human *FGF21*, sense 5′-AAGCCGGGAGTTATTCAAATCTT-3′ and antisense 5′-GTGTGGGGACTTGTTCCCT-3′; human *FGF1*, sense 5′-ACACCGACGGGCTTTTATACG-3′ and antisense 5′-CCCATTCTTCTTGAGGCCAAC-3′; mouse *Atf4* and human *ATF4*, sense 5′-CCTTCGACCAGTCGGGTTTG-3′ and antisense 5′-CTGTCCCGGAAAAGGCATCC-3′; mouse *Ffgr1*, sense 5′-CTGAAGGAGGGTCATCGAAT-3′ and antisense 5′-GTCCAGGTCTTCCACCAACT-3′; mouse *Ffgr2*, sense 5′-CACCACGGACAAAGAGATTG-3′ and antisense 5′-TGTCAACCATGCAGAGTGAA-3′; mouse *Ffgr3*, sense 5′-AGATGCTGAAAGATGATGCG-3′ and antisense 5′-ATGATGTTCTTGTGCTTGCC-3′; mouse *Ffgr4*, sense 5′-CAGAGGCCTTTGGTATGGAT-3′ and antisense 5′-AGGTCTGCCAAATCCTTGTC-3′; and mouse *Klb*, sense 5′-CAGAGAAGGAGGAGGTGAGG-3′ and antisense 5′-CAGCACCTGCCTTAAGTTGA-3′.

Luciferase Reporter Assays—The luciferase (Luc) reporter plasmids for the mouse *Fgf21* promoter spanning the region from −1983 to +5 (WT) and its deletion mutant version (ΔCCACG) were constructed in pGL3 (Promega) utilizing a PCR-based cloning strategy. For luciferase activity assays, 293T cells were co-transfected with the *Fgf21* promoter-Luc and β-galactosidase plasmids before treatment with thapsigargin (1 μM) or tunicamycin (10 μg/ml) for 6 h or co-transfected with the Luc reporter plasmid, pCMV-XBP1s and β-galactosidase plasmids. Luciferase activity was measured using Dual-Luciferase™ reporter assay system (Promega) following the manufacturer's instructions, and β-galactosidase activity was used for normalization.

Chromatin Immunoprecipitation (ChIP)—ChIP assays were performed with the agarose ChIP kit (Pierce) according to the manufacturer's instructions. Cells or liver tissues were subjected to cross-linking with 1% formaldehyde. Glycine solution was then added, and nuclear extracts were prepared. Chromatin-XBP1s complexes were immunoprecipitated with normal rabbit IgG or anti-XBP1s antibodies by incubation at 4 °C overnight on a rocking platform, followed by incubation with the beads from the ChIP kit (Pierce) or protein G-Sepharose beads (GE Healthcare) at 4 °C for 1 h with gentle rocking. After washing five times with the washing buffer, the complexes were eluted with the elution buffer from the beads and were subjected to PCR analysis using the oligonucleotide primers that correspond to the −280 to −24 region of the mouse *Fgf21* promoter as follows: sense 5′-CTCAGACCAAGGAGCACAGA-3′ and antisense 5′-TGAACGCAGAAATACCAGAAT-3′. Regular PCR was conducted with TaKaRa Taq kits (Takara), and real time quantitative PCR was performed with the SYBR Green PCR system (Applied Biosystems).

Statistical Analysis—Data are presented as the mean ± S.E. Statistical analysis was performed using unpaired two-tailed *t* test and one-way or two-way analysis of variance (ANOVA) followed by Bonferroni's post test with GraphPad Prism 4.0. $p < 0.05$ was considered statistically significant.

RESULTS

Hepatic FGF21 Expression Is Associated with ER Stress and Hepatic Steatosis—To investigate whether hepatic FGF21 expression was linked to ER stress during the development of hepatic steatosis, we employed a diet-induced mouse model of

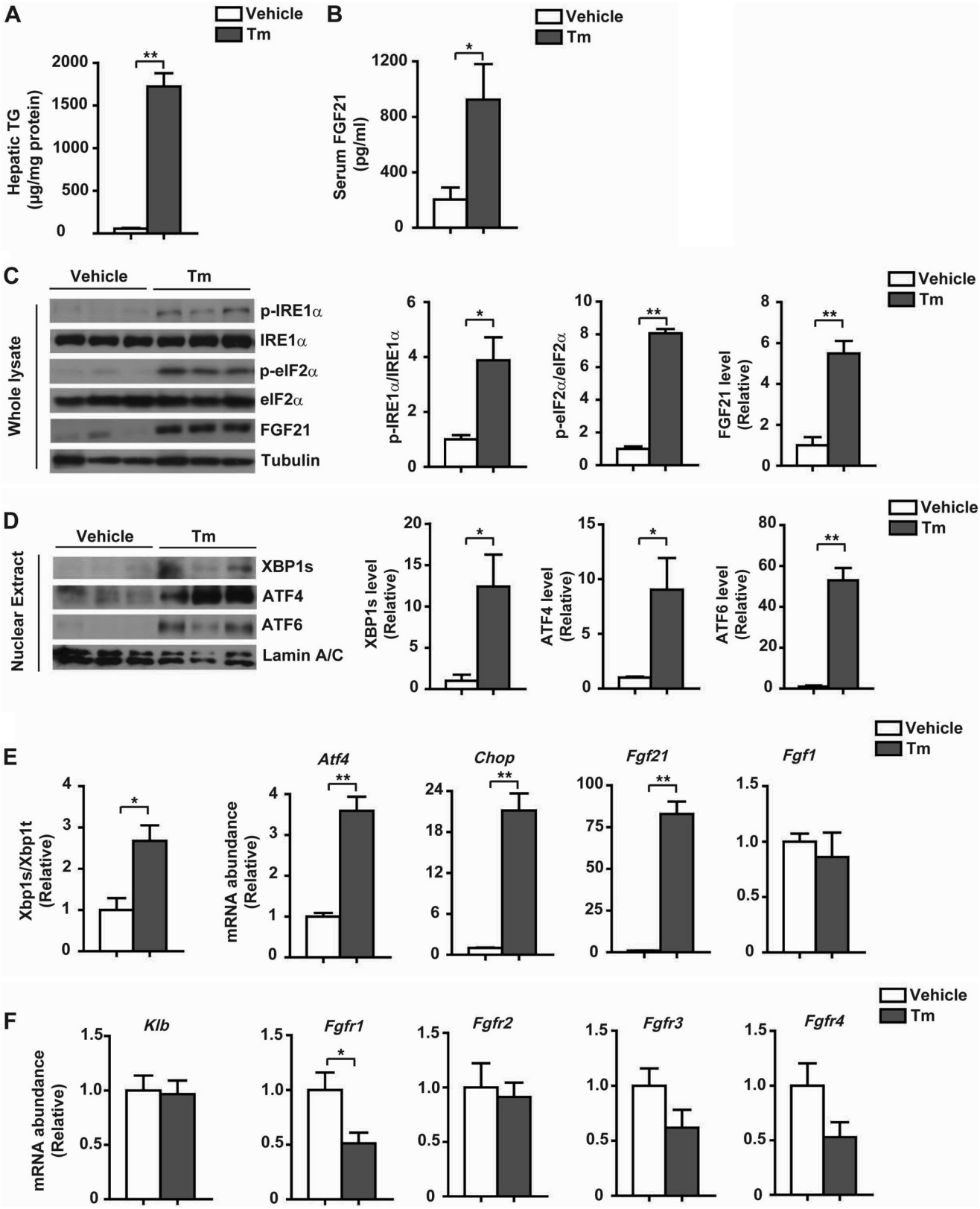

obesity. When fed a high fat diet (HFD) for 16 weeks, mice displayed significant increases in body weight and liver content of triglycerides (TG) relative to control mice fed a low fat diet (LFD) (Fig. 1*A*). HFD-fed mice also had significantly elevated serum levels of FGF21 (Fig. 1*B*). Immunoblotting analyses showed that FGF21 protein levels were increased in livers of HFD-fed obese mice, which were accompanied by increased phosphorylation of IRE1α and eIF2α (Fig. 1*C*), along with increased nuclear accumulation of XBP1s, ATF4, and ATF6 proteins (Fig. 1*D*). Consistently, the splicing of *Xbp1* mRNA and the mRNA abundance of *Atf4* and *Chop* were significantly increased in livers of HFD-fed mice, in parallel with up-regulated mRNA expression of *Fgf21* but not *Fgf1* (Fig. 1*E*). Similarly, activation of all the three UPR branches was also detected in livers of human NAFLD patients when compared with those of control subjects without NAFLD (Fig. 2, *A–C*), and this was accompanied by increased levels of FGF21 protein (Fig. 2*A*) and *FGF21* mRNA (Fig. 2*C*). These results demonstrated the occurrence of metabolic ER stress during hepatic steatosis, which was associated with the up-regulation of hepatic FGF21 expression in both animals and humans.

Expression of FGF21 Is Induced upon Experimental ER Stress—To determine whether FGF21 expression is directly linked to ER stress, we first treated HepG2 cells for different time intervals with tunicamycin and thapsigargin, the two chemical ER stressors. Both tunicamycin and thapsigargin caused activation of the UPR, including increases in IRE1α phosphorylation and XBP1s protein abundance (Fig. 3*A*), greater accumulation of nuclear ATF6 and ATF4 proteins (Fig. 3*A*), and elevations in the splicing of *XBP1* mRNA (Fig. 3*B*) and the mRNA abundance of *ATF4* and *CHOP* (Fig. 3*C*). Tunicamycin or thapsigargin also resulted in increased levels of FGF21 protein (Fig. 3*A*), along with elevated mRNA abundance of *FGF21* but not *FGF1* (Fig. 3*C*). Consistently, higher secreted FGF21 protein levels were detected from the culture medium of HepG2 cells treated with tunicamycin or thapsigargin (Fig. 3*D*). Next, we treated mice with tunicamycin for 24 h, which caused marked increases in liver TG content (Fig. 4*A*) and serum levels of FGF21 (Fig. 4*B*). Tunicamycin activated the three UPR branches in the liver (Fig. 4, *C* and *D*), while prominently increasing the level of hepatic FGF21 protein (Fig. 4*C*) as well as the *Fgf21* mRNA abundance (Fig. 4*E*). Thus, hepatic FGF21 expression could be induced under experimental ER stress conditions both *in vitro* and *in vivo*. Notably, tunicamycin treatment resulted in considerable decreases in liver mRNA levels of FGFR1, -3, and -4 (Fig. 4*F*), the potential FGF21 receptors (49, 50), without influencing the expression of β-klotho, the co-factor required for FGF21 activity (51). These results indicate that ER stress might attenuate FGF21 signaling through down-regulating its receptor expression. In addition, we also observed

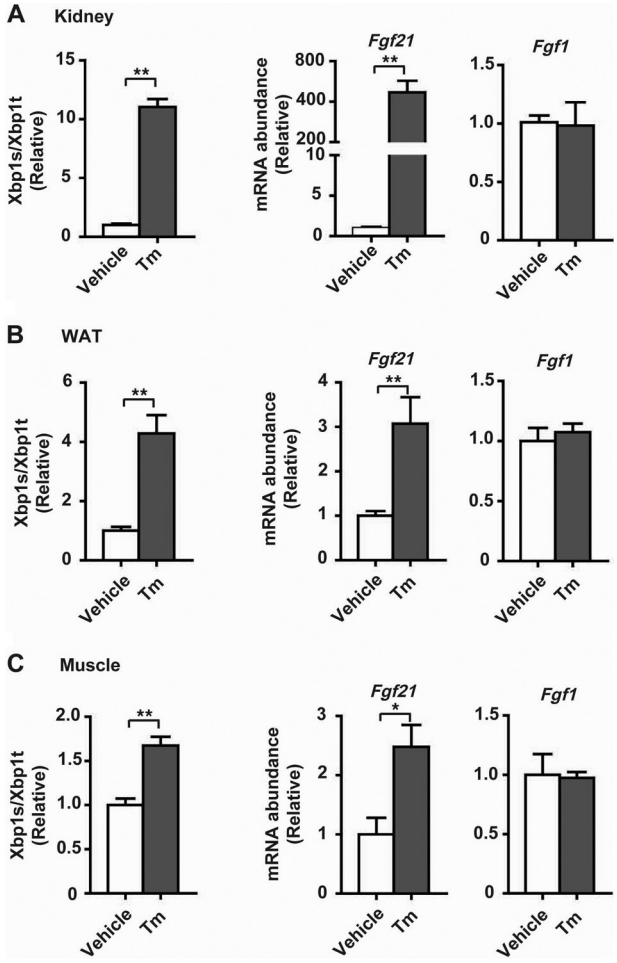

FIGUR 5. **ER stress induces the expression of FGF21 in kidney, white adipose tissue, and muscle.** Mice were treated with PBS (vehicle) or Tm for 24 h. *Xbp1* mRNA splicing and the mRNA abundance of *Fgf21* and *Fgf1* in kidney (*A*), fat tissue (*B*), and muscle (*C*) were determined by quantitative RT-PCR. Data were normalized to the values of the vehicle control group and are presented as mean ± S.E. ($n = 5$/group). *, $p < 0.05$; **, $p < 0.01$ by *t* test.

elevations in the mRNA abundance of *Fgf21* in the kidney, white adipose tissue, and muscle of tunicamycin-treated mice (Fig. 5, *A–C*). This implies that FGF21 is also likely to exert cytoprotective functions in other tissues such as the kidney, an organ that can be very sensitive to ER stress.

IRE1α-XBP1 Pathway Regulates the Transcriptional Expression of Fgf21—Given that FGF21 was reported as an ATF4-regulated gene (42, 43), we tested whether FGF21 is a common downstream target of multiple UPR pathways using liver-specific IRE1α knock-out (LKO) mice that we created (44). Interestingly, when compared with *flox/flox* control mice, tunicamycin-treated LKO mice had lower serum FGF21 levels (Fig. 6*A*). In primary hepatocytes, hepatic IRE1α deficiency not only

FIGUR 4. **ER stress causes liver steatosis with up-regulated expression of hepatic FGF21 in mice.** Male C57BL/6 mice at 12 weeks of age were treated for 24 h through intraperitoneal injection with PBS (vehicle) or Tm (1 mg/kg body weight). *A,* liver triglycerides were determined. *B,* serum levels of FGF21 were measured. Data are shown as the mean ± S.E. ($n = 5$/group). *, $p < 0.05$; **, $p < 0.01$ by *t* test. *C,* immunoblot analyses of the UPR markers, including p-IRE1α and p-eIF2α, and FGF21 protein abundance in whole liver lysates. Representative results are shown for three individual mice per group. Ratios of p-IRE1α/IRE1α and p-eIF2α/eIF2α as well as FGF21 protein levels were quantified. *D,* immunoblot analyses of nuclear XBP1s, ATF4, and ATF6 protein levels. Representative results are shown for three individual mice per group, and quantitation was done by normalization to lamin A/C. *E, Xbp1* mRNA splicing and the mRNA abundance of *Atf4*, *Chop*, *Fgf21,* and *Fgf1* were analyzed by quantitative RT-PCR. *F,* analysis by quantitative RT-PCR of the mRNA abundance of the FGF21 receptors *Klb, Fgfr1, Fgfr2, Fgfr3*, and *Fgfr4*. Data in *C–F* were normalized to the values of the vehicle control group and are presented as mean ± S.E. ($n = 5$/group). *, $p < 0.05$; **, $p < 0.01$ by *t* test.

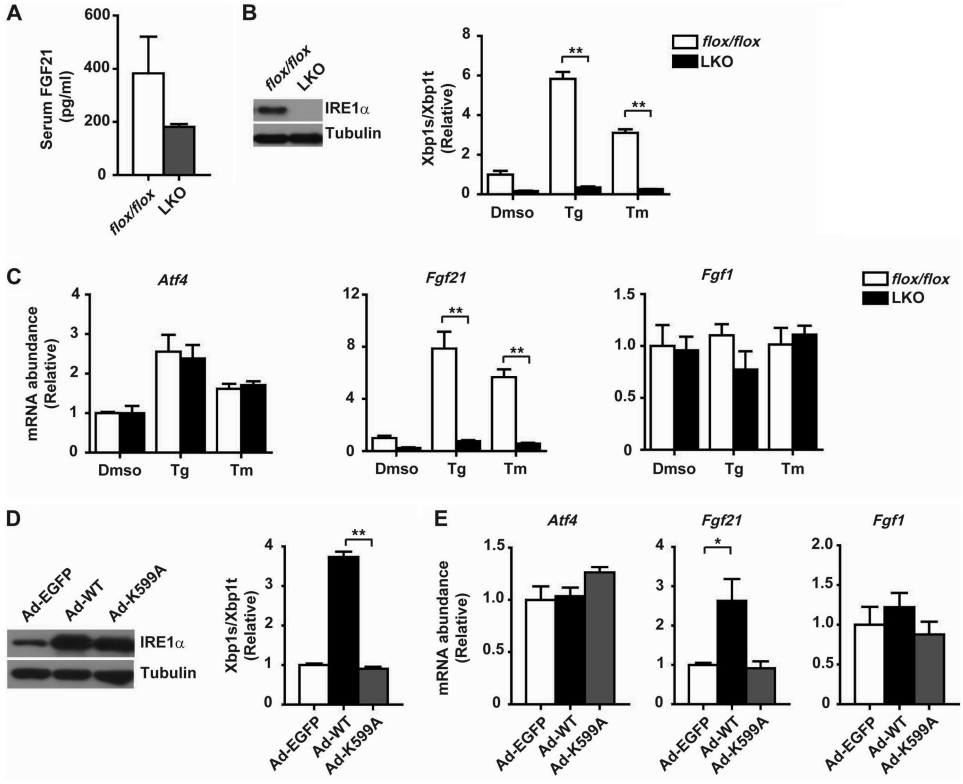

FIGURE 6. **IRE1α is responsible for ER stress-induced expression of FGF21 in hepatocytes.** *A,* male *flox/flox* or IRE1α null *LKO* mice were treated with tunicamycin (1 mg/kg body weight) for 8 h. Serum levels of FGF21 were measured and are shown as the mean ± S.E. ($n = 3$/group). *B* and *C,* primary hepatocytes from male *flox/flox* or *LKO* mice were treated for 6 h with dimethyl sulfoxide (*DMSO*), thapsigargin (*Tg*, 1 μM), or Tm (10 μg/ml). *B,* immunoblot analysis of IRE1α protein expression and quantitative RT-PCR analysis of *Xbp1* mRNA splicing. *C,* analyses of the mRNA abundance of *Atf4*, *Fgf21*, and *Fgf1*. Data were normalized to values of DMSO-treated *flox/flox* hepatocytes and are shown as the mean ± S.E. ($n = 3$ independent experiments). **, $p < 0.01$ by two-way ANOVA. *D* and *E,* primary hepatocytes from male C57BL/6 mice were infected for 2 days with adenoviruses expressing EGFP or the wild-type (*WT*) or kinase-dead K599A mutant human IRE1α protein. *D,* immunoblot analysis of IRE1α and quantitative RT-PCR analysis of *Xbp1* mRNA splicing. *E,* analyses of the mRNA abundance of the indicated genes. Data were normalized to values from Ad-EGFP control cells and are shown as the mean ± S.E. ($n = 3$ independent experiments). *, $p < 0.05$; **, $p < 0.01$ by one-way ANOVA.

completely abolished tunicamycin- or thapsigargin-induced *Xbp1* mRNA splicing (Fig. 6*B*), it also markedly diminished ER stress induction of *Fgf21* without affecting the expression of *Atf4* or *Fgf1* (Fig. 6*C*). Conversely, adenovirus-mediated overexpression in hepatocytes of the wild-type (WT) but not the kinase-dead K599A mutant IRE1α could significantly increase the splicing of the *Xbp1* mRNA (Fig. 6*D*) and the mRNA abundance of *Fgf21* (Fig. 6*E*). Next, to determine whether IRE1α regulation of *Fgf21* expression is indeed mediated by XBP1s, we employed adenovirus-expressed shRNA to knock down the expression of XBP1 in primary hepatocytes (Fig. 7*A*). This resulted in significant reductions in ER stress-induced expression of *Fgf21* but not *Atf4* or *Fgf1* (Fig. 7*B*). Conversely, adenoviral overexpression of XBP1s (Fig. 7*C*) greatly increased the expression of *Fgf21* but did not affect the expression of *Atf4* or *Fgf1* (Fig. 7*D*). These data demonstrate that the IRE1α-XBP1 branch of the UPR plays a crucial role in regulation of FGF21 expression in response to ER stress.

We then examined whether *Fgf21* is a direct transcriptional target of XBP1s. Luciferase reporter assays showed that the mouse *Fgf21* promoter could be activated under experimental ER stress conditions (Fig. 8*A*). Moreover, a putative ER stress-response element (ERSE), CCATT . . . N(*n*) . . . CCACG, was identified, a potential XBP1s-binding core site (52) that is also conserved in the promoter of human and rat *Fgf21* genes (Fig. 8*B*). Importantly, XBP1s co-expression stimulated the mouse *Fgf21* promoter activity, and deletion of CCACG from this ERSE abolished the ability of XBP1s to stimulate it (Fig. 8*C*). Chromatin immunoprecipitation (ChIP) assays showed that XBP1s physically bound to the ERSE-containing region of the *Fgf21* promoter (Fig. 8*D*), and the CCACG core sequence was required for its binding (Fig. 8*E*). Next, we determined through ChIP assays whether endogenous XBP1s could bind to the *Fgf21* promoter in an ER stress-responsive manner *in vivo*. Indeed, tunicamycin treatment significantly increased XBP1s occupancy of the *Fgf21* promoter in the livers of mice (Fig. 8*F*). These results reveal that the IRE1α-XBP1 pathway drives the transcriptional expression of *Fgf21* during ER stress. Therefore, *Fgf21* serves as a downstream target gene of the UPR, which is regulated dually by ATF4 and XBP1s.

FGF21-ERK Signaling Suppresses the eIF2α-ATF4-CHOP Pathway of ER Stress—The observed UPR-responsive expression of FGF21 suggests that FGF21 may act as a UPR effector to exert feedback effects on ER stress-associated metabolic changes. To test this idea, we first examined the effect of recombinant mouse FGF21 protein upon tunicamycin-induced ER stress signaling in mouse primary hepatocytes. Notably, FGF21 treatment did not cause significant changes in tunicamycin-induced phosphorylation of IRE1α (Fig. 9*A*) or splicing of *Xbp1* mRNA (Fig. 9*B*), but it significantly decreased the phosphory-

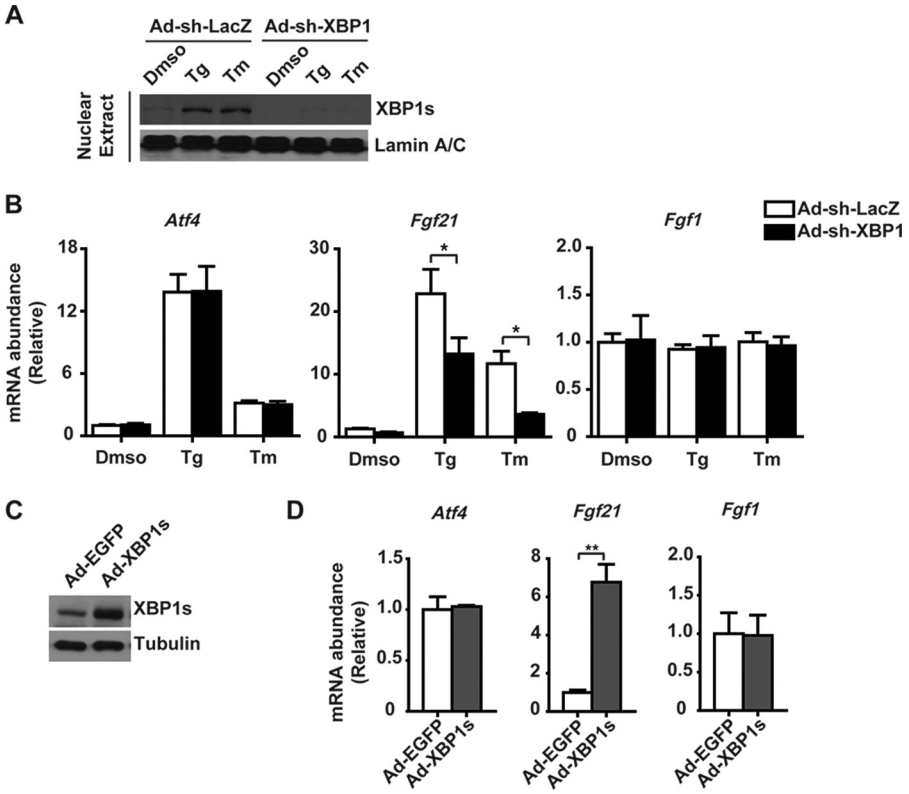

FIGURE 7. **XBP1s mediates ER stress-induced expression of FGF21 in hepatocytes.** *A* and *B,* primary hepatocytes from male C57BL/6 mice were infected for 3 days with adenoviruses expressing a short hairpin (*sh*) RNA directed against LacZ (*Ad-shLacZ*) or XBP1 (*Ad-shXBP1*) before treatment for 6 h with DMSO, thapsigargin (*Tg*), or Tm. *A,* immunoblot analysis of XBP1s protein from nuclear extracts. *B,* analyses by quantitative RT-PCR of the mRNA abundance of the indicated genes. Results were normalized to values from DMSO-treated cells infected with Ad-shLacZ and are shown as the mean ± S.E. ($n = 3$ independent experiments). *, $p < 0.05$ by two-way ANOVA. *C* and *D,* primary hepatocytes were infected for 2 days with adenoviruses expressing EGFP or XPB1s protein. *C,* immunoblot analysis of XBP1s protein from cell lysates. *D,* quantitative RT-PCR analyses of the mRNA abundance of the indicated genes. Data were normalized to values from Ad-EGFP control cells and are shown as the mean ± S.E. ($n = 3$ independent experiments). **, $p < 0.01$ by *t* test.

lation of eIF2α (Fig. 9*A*) and the mRNA abundance of *Atf4* and *Chop* (Fig. 9*B*), leading to a reduced protein level of CHOP (Fig. 9*C*). To determine the possible mechanism that mediates FGF21's actions, we examined whether FGF21-induced MAPK phosphorylation (29, 33) is involved. During tunicamycin-induced ER stress in hepatocytes, FGF21 treatment increased ERK phosphorylation (Fig. 10*A*), which was markedly inhibited by U0126, a chemical ERK inhibitor. Importantly, suppression of ERK activation significantly blunted the attenuating effects of FGF21 upon tunicamycin-induced eIF2α phosphorylation and CHOP expression (Fig. 10, *A–C*). These data indicate that FGF21-directed ERK activation likely mediates its actions in counteracting ER stress, leading to suppression of the eIF2α-ATF4-CHOP pathway.

FGF21 Alleviates ER Stress-induced Hepatic Steatosis—We then analyzed the metabolic effects of FGF21 in tunicamycin-treated mice. Tunicamycin caused a marked increase in hepatic TG content but a prominent decrease in serum TG levels (Fig. 11*A*), which likely resulted from suppression of hepatic TG secretion and/or enhanced liver TG biosynthesis/uptake. Interestingly, although causing considerable reductions in both hepatic and serum TG levels in the absence of tunicamycin treatment, FGF21 administration in tunicamycin-treated mice resulted in a significant decrease in hepatic TG overload (Fig. 11*A*, *left panel*), but it did not affect the reduction of serum TG levels (Fig. 11*A*, *right panel*). This indicates that FGF21 had little effect upon tunicamycin-elicited changes in hepatic TG secretion or uptake. Similar to the observations in hepatocytes, FGF21 showed insignificant effect upon the phosphorylation of IRE1α (Fig. 11*B*) or splicing of *Xbp1* mRNA (Fig. 11*C*) in the livers of tunicamycin-treated mice, but it substantially blocked the phosphorylation of eIF2α (Fig. 11*B*) and significantly blunted the elevations in the mRNA abundance of *Atf4* and *Chop* (Fig. 11*C*). ER stress has been shown to enhance *de novo* lipid biosynthesis via activation of SREBP1 proteins (22, 23, 53), and we observed that FGF21 administration resulted in appreciable decreases in matured SREBP1 protein levels in livers of tunicamycin-treated mice (Fig. 11*D*). Given that CHOP is viewed as a transcriptional repressor that is implicated in the disruption of metabolic networks (22), these results suggest that FGF21 may suppress the eIF2α-ATF4-CHOP pathway, thereby counteracting ER stress to ameliorate hepatic steatosis through reducing lipogenesis while promoting lipid oxidation.

DISCUSSION

Many studies have established the importance of FGF21 that functions as a hormone to regulate carbohydrate and lipid metabolism (24). Despite its remarkable pharmacological beneficial effects in improving metabolic parameters

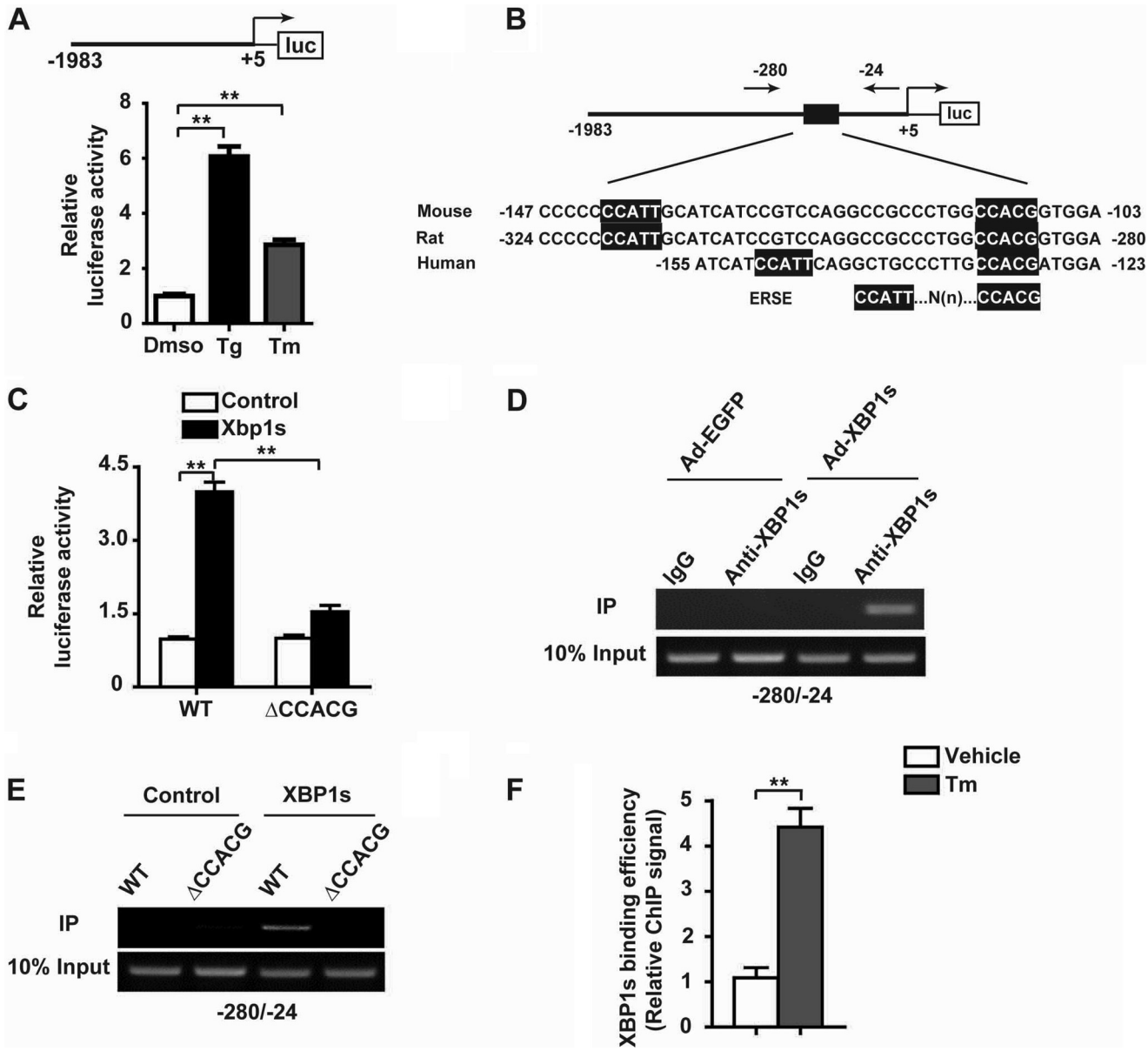

FIGURE 8. **XBP1s transactivates the transcriptional activity of the *Fgf21* promoter.** *A,* luciferase reporter assay. 293T cells were transfected with the Luc construct under the control of the mouse *Fgf21* promoter that spans the region from −1983 to +5. Cells were then treated with DMSO, thapsigargin (*Tg*), or Tm for 6 h. Data were normalized to the DMSO control and are shown as the mean ± S.E. ($n = 3$ independent experiments). **, $p < 0.01$ by one-way ANOVA. *B,* sequence comparison of mouse, rat, and human *Fgf21* promoter. Shown is the region that contains the signature XBP1s-binding element (ERSE) indicated by *black boxes*. *C,* luciferase reporter assay. 293T cells were co-transfected with the empty control vector or pCMV-XBP1s plasmid together with Luc constructs under the control of the mouse *Fgf21* promoter (WT) or that with the CCACG element deleted (ΔCCACG). Data are shown as the mean ± S.E. ($n = 3$ independent experiments). **, $p < 0.01$ by two-way ANOVA. *D,* chromatin immunoprecipitation (*IP*) assay. Primary hepatocytes were infected for 2 days with adenoviruses expressing EGFP or XBP1s. ChIP was performed using control IgG or XBP1s antibody prior to PCR amplification of the indicated region (nucleotide −280 to −24) of the promoter. *E,* ChIP assay of extracts from 293T cells co-transfected with the empty control vector or pCMV-XBP1s plasmid together with the WT or ΔCCACG mutant reporter construct. ChIP was performed using anti-XBP1s antibody. *F,* ChIP assay of liver nuclear extracts from male C57BL/6 mice treated with PBS (vehicle) or Tm (1 mg/kg body weight) using control IgG or anti-XBP1s antibody. Quantitative PCR results are shown as the mean ± S.E. ($n = 5$/group). **, $p < 0.01$ by two-way ANOVA.

such as body weight, insulin sensitivity, and hyperlipidemia, increased circulating levels of FGF21 have been shown to be associated with human obesity, type 2 diabetes, and NAFLD (34–40). It remains largely elusive how changes in FGF21 expression are linked to the pathogenic development of metabolic disorders. In this study, we found in both mice and human subjects that hepatic FGF21 expression is coupled to cellular ER stress response in the face of NAFLD. Furthermore, our results suggest that FGF21 can be dually regulated by the IRE1α-XBP1 and eIF2α-ATF4 pathways (Fig. 11*E*) and can serve as a direct downstream target of the UPR program; FGF21 can in turn counteract ER stress to alleviate hepatic steatosis.

ER stress is thought to underlie metabolic dysfunctions (13–15), and the three UPR pathways have been implicated in various metabolic processes (3, 12). As a hepatokine, FGF21 expression is responsive to nutritional states (24), and animal model studies have shown that hepatic FGF21 is transcriptionally controlled by the nuclear receptor PPARα

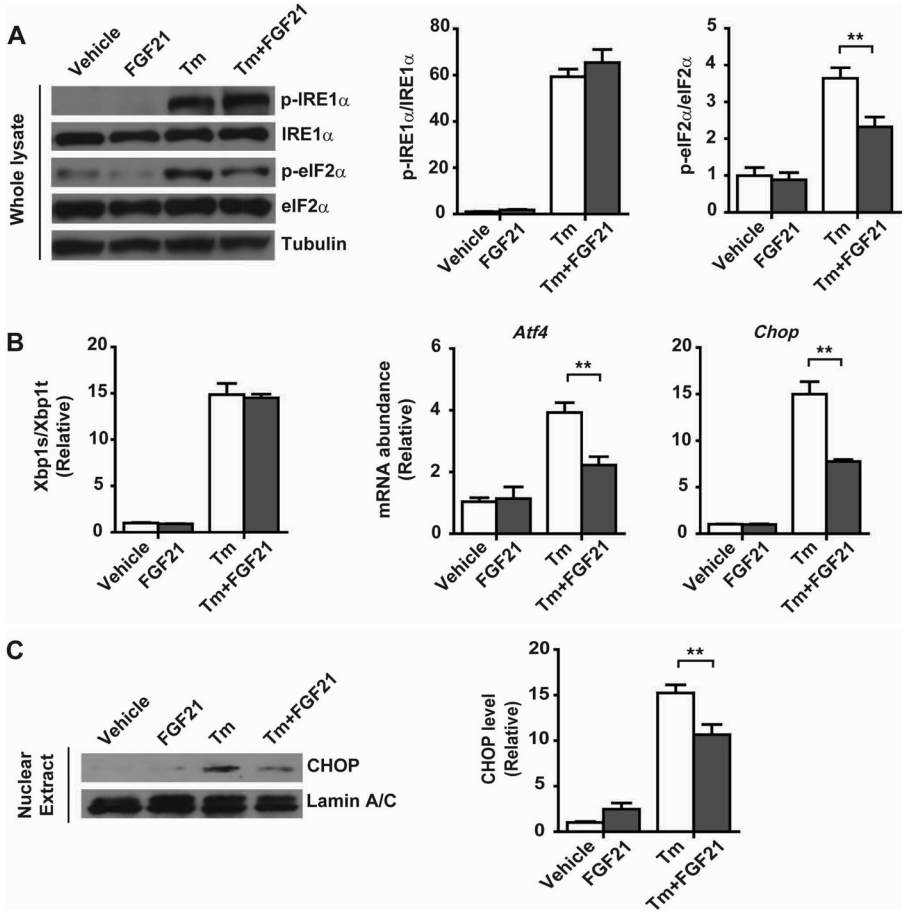

FIGURE 9. **Recombinant FGF21 protein suppresses the eIF2α-ATF4-CHOP pathway during ER stress in hepatocytes.** Primary hepatocytes were isolated from male C57BL/6 mice and treated with DMSO (vehicle), recombinant mouse FGF21 (1 μg/ml), Tm (10 μg/ml), or tunicamycin after pretreatment with FGF21. *A,* immunoblotting of p-IRE1α, p-eIF2α, IRE1α, and eIF2α. Tubulin was used as the loading control. Ratios of p-IRE1α/IRE1α and p-eIF2α/eIF2α were quantified ($n = 3$ independent experiments). *B,* quantitative RT-PCR analyses of *Xbp1* mRNA splicing and the mRNA abundance of *Atf4* and *Chop* ($n = 3$ independent experiments). *C,* immunoblotting of CHOP protein in nuclear extracts. Lamin A/C was used as the loading control. CHOP protein levels were quantified and normalized to lamin A/C ($n = 3$ independent experiments). Data were normalized to the values of the vehicle control group and are presented as mean ± S.E. **, $p < 0.01$ by two-way ANOVA.

during prolonged starvation (25, 26). We previously showed that the IRE1α pathway is activated in the liver during fasting or starvation (44, 47). Hepatic IRE1α can sense nutrient deprivation and regulate the adaptive shift of fuel utilization through XBP1s-directed regulation of PPARα. In this scenario, metabolic activation of the IRE1α-XBP1 pathway promotes the expression of *Fgf21* as a PPARα target gene, indicating a physiological role for the IRE1α-XBP1 branch in the starvation response. Our findings herein suggest that XBP1s may also directly up-regulate *Fgf21* in a PPARα-independent manner during prolonged fasting. Although XBP1 has been implicated in the regulation of lipogenesis (54), XBP1s-mediated up-regulation of *Fgf21* likely represents a feedback mechanism to control liver TG content through lipid oxidation. Under ER stress conditions, the transcriptional expression of *Fgf21* is not only up-regulated by XBP1s but also by ATF4 (42, 43), and this dual induction indicates that FGF21 is a *bona fide* effector of the UPR program. The fact that FGF21 expression is controlled by at least two of the three UPR signaling arms not only supports an important role for FGF21 in the feedback control of ER stress responses, it also reflect the coordinated feature of multiple UPR arms in exerting their metabolic actions.

Our results from tunicamycin-treated mice showed that administration of recombinant FGF21 could ameliorate hepatic TG overload that was caused by typical ER stress. Interestingly, this was associated with suppression by FGF21 of both the eIF2α-ATF4-CHOP pathway of ER stress and ER stress-activated SREBP1 protein maturation. CHOP has been shown to suppress metabolic genes through disrupting the function of C/EBPα, consequently leading to perturbations of fatty acid oxidation, lipoprotein secretion, and other metabolic processes (22). Thus, FGF21-induced suppression of CHOP expression may constitute a possibly major mechanism that mediates its alleviating effect upon liver steatosis during ER stress. Although it remains to be more clearly delineated how FGF21 signaling is mechanistically linked to maintaining ER homeostasis or suppressing the PERK-eIF2α-CHOP pathway, our results indicate that FGF21-induced ERK activation contributes to mediating the feedback effect of FGF21 upon ER stress. Moreover, it is worth further dissecting whether FGF21 can exert similar effects upon liver steatosis through mitigating obesity-related

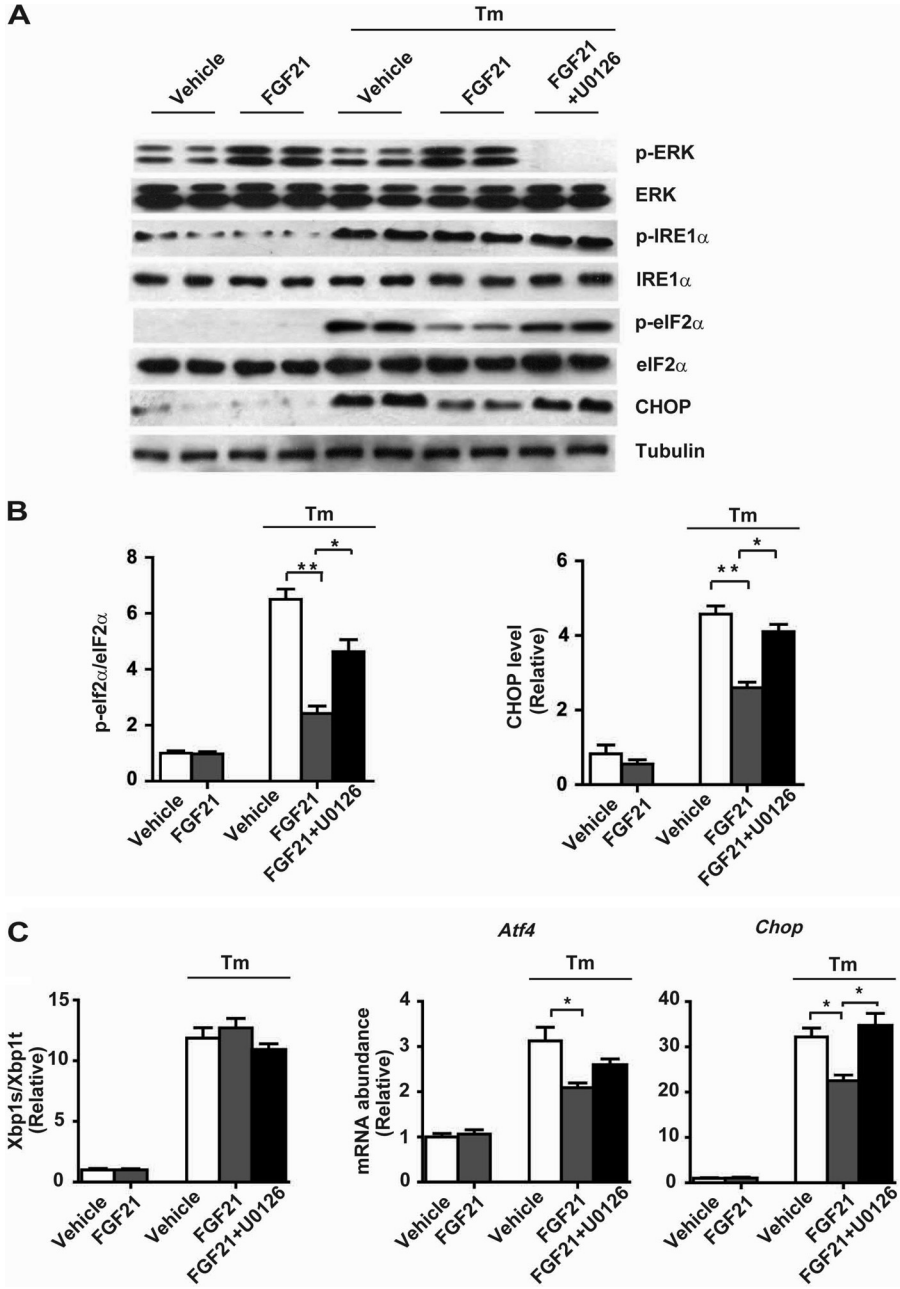

FIGURE 10. **Inhibition of ERK activation blunts the suppressive effect of FGF21 on the eIF2α-ATF4-CHOP pathway.** Primary hepatocytes were treated with DMSO (vehicle), recombinant mouse FGF21 (1 μg/ml), Tm (10 μg/ml), or tunicamycin after pretreatment with FGF21 in the absence or presence of ERK inhibitor U0126 as indicated. *A,* immunoblotting of p-ERK, ERK, p-IRE1α, IRE1α, p-eIF2α, eIF2α, and CHOP. Tubulin was used as the loading control. *B,* ratios of p-eIF2α/eIF2α and CHOP protein levels were quantified ($n = 3$ independent experiments). *C,* quantitative RT-PCR analyses of *Xbp1* mRNA splicing and the mRNA abundance of *Atf4* and *Chop* ($n = 3$ independent experiments). Data were normalized to the values of vehicle control group and are shown as the mean ± S.E. *, $p < 0.05$; **, $p < 0.01$ by two-way ANOVA.

metabolic ER stress. In addition to modulating lipid metabolism in the liver, the suppressive effect of the FGF21-ERK pathway upon the expression of CHOP implies that FGF21 may also influence ER stress-induced apoptosis, like another FGF family member FGF2 (55). Indeed, we also noticed an alleviating effect of FGF21 upon tunicamycin-induced apoptosis in cultured cells (data not shown), indicating a broader range of functions of FGF21 under ER stress-associated conditions.

In summary, our findings reveal that FGF21 is functionally linked to ER stress in the state of hepatic steatosis. The expression of FGF21 is controlled by dual branches of the UPR, *i.e.* ATF4 and XBP1s. This suggests that FGF21 can act as an integral component of the cellular UPR program in the management of ER stress. It is worth noting that FGF21 was recently shown to exert its metabolic actions in adipose tissues in an autocrine fashion (56–58) and could even function as a myokine (43). Given that increased ER stress is found to occur in the liver as well as in the adipose tissues and muscles, it remains to be elucidated whether FGF21 can act as a UPR effector to affect the functions of other metabolic tissues besides the liver. In addition, it is also tempting to speculate that FGF21, as a component of the UPR pro-

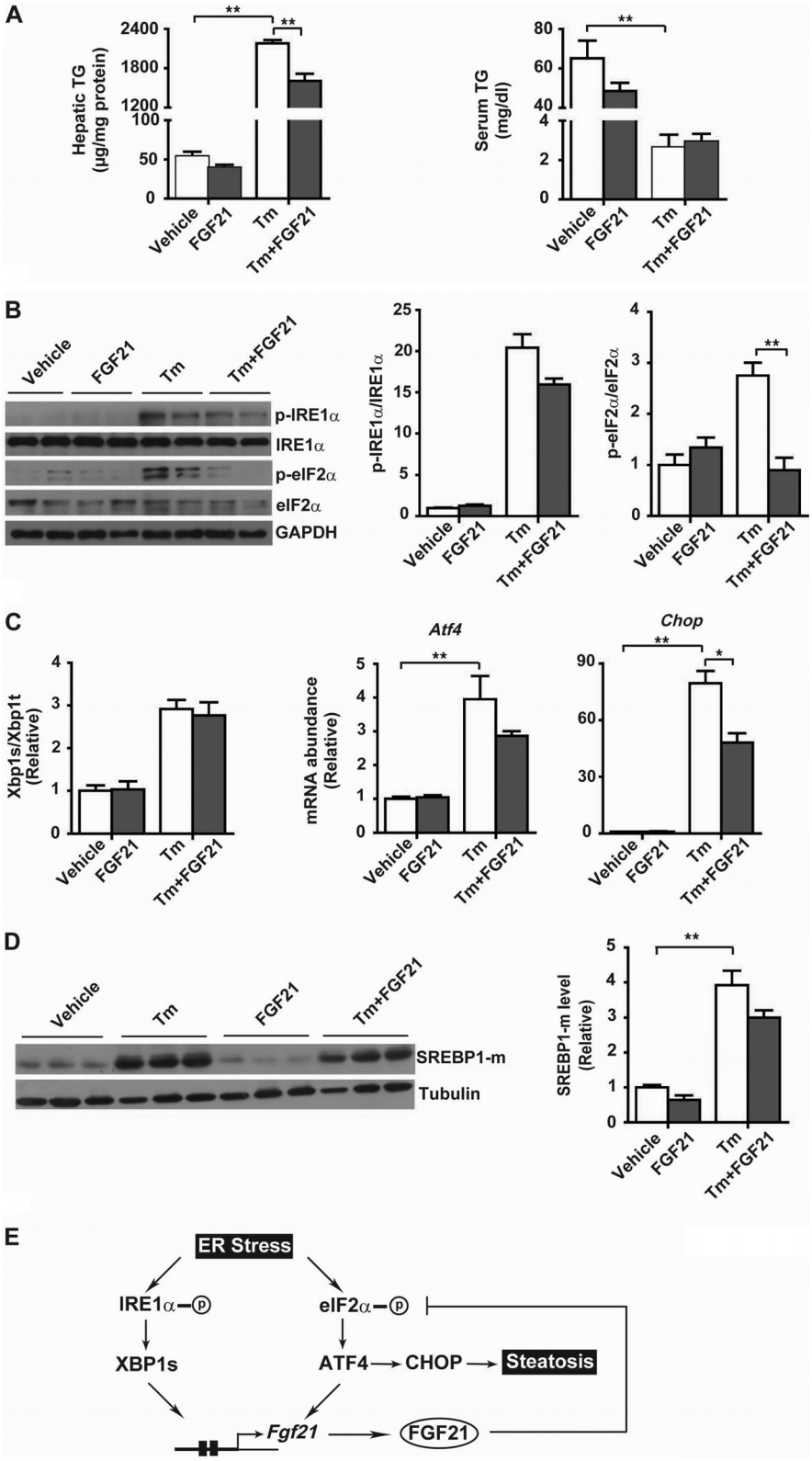

FIGURE 11. **Administration of FGF21 reduces ER stress-induced hepatic steatosis in mice.** Male C57BL/6 mice at 12 weeks of age were injected intraperitoneally with PBS (vehicle) or recombinant mouse FGF21 (1 mg/kg body weight) together with DMSO (vehicle) or Tm (1 mg/kg body weight) ($n = 5$/group). Mice were sacrificed at 24 h after treatment. *A,* liver TG contents and serum TG levels. *B,* immunoblot analysis of p-IRE1α, p-eIF2α, IRE1α, and eIF2α in whole liver lysates. GAPDH was used as the loading control. Representative results are shown for two individual mice per group. Ratios of p-IRE1α/IRE1α and p-eIF2α/eIF2α were quantified and are presented as the mean ± S.E. ($n = 5$/group). *C,* quantitative RT-PCR analyses of *Xbp1* mRNA splicing and the mRNA abundance of *Atf4* and *Chop*. Data are shown as the mean ± S.E. ($n = 5$/group). *D,* immunoblot analysis of matured SREBP1 protein (*SREBP1-m*) in whole liver lysates. Tubulin was used as the loading control. SREBP1-m levels were quantified and normalized to tubulin ($n = 5$/group). Data in *B–D* were normalized to the values of the vehicle control mice. *, $p < 0.05$; **, $p < 0.01$ by two-way ANOVA. *E,* schematic model. Dually controlled by XBP1s and ATF4, FGF21 acts in turn to suppress the eIF2α-ATF4-CHOP pathway and alleviate ER stress-induced hepatic steatosis.

gram, may exert beneficial actions in other ER stress-associated pathologies.

Acknowledgment—We thank Dr. Ling Qi (Cornell University) for providing the recombinant adenoviruses for the knockdown of XBP1 and overexpression of XBP1s.

REFERENCES

1. Ron, D., and Walter, P. (2007) Signal integration in the endoplasmic reticulum unfolded protein response. *Nat. Rev. Mol. Cell Biol.* **8,** 519–529
2. Walter, P., and Ron, D. (2011) The unfolded protein response: from stress pathway to homeostatic regulation. *Science* **334,** 1081–1086
3. Fu, S., Watkins, S. M., and Hotamisligil, G. S. (2012) The role of endoplasmic reticulum in hepatic lipid homeostasis and stress signaling. *Cell Metab.* **15,** 623–634
4. Cox, J. S., Shamu, C. E., and Walter, P. (1993) Transcriptional induction of genes encoding endoplasmic reticulum resident proteins requires a transmembrane protein kinase. *Cell* **73,** 1197–1206
5. Sidrauski, C., and Walter, P. (1997) The transmembrane kinase Ire1p is a site-specific endonuclease that initiates mRNA splicing in the unfolded protein response. *Cell* **90,** 1031–1039
6. Shamu, C. E., and Walter, P. (1996) Oligomerization and phosphorylation of the Ire1p kinase during intracellular signaling from the endoplasmic reticulum to the nucleus. *EMBO J.* **15,** 3028–3039
7. Welihinda, A. A., and Kaufman, R. J. (1996) The unfolded protein response pathway in *Saccharomyces cerevisiae*. Oligomerization and transphosphorylation of Ire1p (Ern1p) are required for kinase activation. *J. Biol. Chem.* **271,** 18181–18187
8. Yoshida, H., Matsui, T., Yamamoto, A., Okada, T., and Mori, K. (2001) XBP1 mRNA is induced by ATF6 and spliced by IRE1 in response to ER stress to produce a highly active transcription factor. *Cell* **107,** 881–891
9. Harding, H. P., Novoa, I., Zhang, Y., Zeng, H., Wek, R., Schapira, M., and Ron, D. (2000) Regulated translation initiation controls stress-induced gene expression in mammalian cells. *Mol. Cell* **6,** 1099–1108
10. Tsaytler, P., Harding, H. P., Ron, D., and Bertolotti, A. (2011) Selective inhibition of a regulatory subunit of protein phosphatase 1 restores proteostasis. *Science* **332,** 91–94
11. Harding, H. P., Zhang, Y., Scheuner, D., Chen, J. J., Kaufman, R. J., and Ron, D. (2009) Ppp1r15 gene knockout reveals an essential role for translation initiation factor 2α (eIF2α) dephosphorylation in mammalian development. *Proc. Natl. Acad. Sci. U.S.A.* **106,** 1832–1837
12. Hetz, C. (2012) The unfolded protein response: controlling cell fate decisions under ER stress and beyond. *Nat. Rev. Mol. Cell Biol.* **13,** 89–102
13. Eizirik, D. L., Cardozo, A. K., and Cnop, M. (2008) The role for endoplasmic reticulum stress in diabetes mellitus. *Endocr. Rev.* **29,** 42–61
14. Hotamisligil, G. S. (2010) Endoplasmic reticulum stress and the inflammatory basis of metabolic disease. *Cell* **140,** 900–917
15. Malhi, H., and Kaufman, R. J. (2011) Endoplasmic reticulum stress in liver disease. *J. Hepatol.* **54,** 795–809
16. Bedogni, G., Miglioli, L., Masutti, F., Tiribelli, C., Marchesini, G., and Bellentani, S. (2005) Prevalence of and risk factors for nonalcoholic fatty liver disease: the Dionysos nutrition and liver study. *Hepatology* **42,** 44–52
17. Rector, R. S., Thyfault, J. P., Wei, Y., and Ibdah, J. A. (2008) Non-alcoholic fatty liver disease and the metabolic syndrome: an update. *World J. Gastroenterol.* **14,** 185–192
18. Das, S. K., Chu, W. S., Mondal, A. K., Sharma, N. K., Kern, P. A., Rasouli, N., and Elbein, S. C. (2008) Effect of pioglitazone treatment on endoplasmic reticulum stress response in human adipose and in palmitate-induced stress in human liver and adipose cell lines. *Am. J. Physiol. Endocrinol. Metab.* **295,** E393–E400
19. Gregor, M. F., Yang, L., Fabbrini, E., Mohammed, B. S., Eagon, J. C., Hotamisligil, G. S., and Klein, S. (2009) Endoplasmic reticulum stress is reduced in tissues of obese subjects after weight loss. *Diabetes* **58,** 693–700
20. Puri, P., Mirshahi, F., Cheung, O., Natarajan, R., Maher, J. W., Kellum, J. M., and Sanyal, A. J. (2008) Activation and dysregulation of the unfolded protein response in nonalcoholic fatty liver disease. *Gastroenterology* **134,** 568–576
21. Sharma, N. K., Das, S. K., Mondal, A. K., Hackney, O. G., Chu, W. S., Kern, P. A., Rasouli, N., Spencer, H. J., Yao-Borengasser, A., and Elbein, S. C. (2008) Endoplasmic reticulum stress markers are associated with obesity in nondiabetic subjects. *J. Clin. Endocrinol. Metab.* **93,** 4532–4541
22. Rutkowski, D. T., Wu, J., Back, S. H., Callaghan, M. U., Ferris, S. P., Iqbal, J., Clark, R., Miao, H., Hassler, J. R., Fornek, J., Katze, M. G., Hussain, M. M., Song, B., Swathirajan, J., Wang, J., Yau, G. D., and Kaufman, R. J. (2008) UPR pathways combine to prevent hepatic steatosis caused by ER stress-mediated suppression of transcriptional master regulators. *Dev. Cell* **15,** 829–840
23. Zhang, K., Wang, S., Malhotra, J., Hassler, J. R., Back, S. H., Wang, G., Chang, L., Xu, W., Miao, H., Leonardi, R., Chen, Y. E., Jackowski, S., and Kaufman, R. J. (2011) The unfolded protein response transducer IRE1α prevents ER stress-induced hepatic steatosis. *EMBO J.* **30,** 1357–1375
24. Potthoff, M. J., Kliewer, S. A., and Mangelsdorf, D. J. (2012) Endocrine fibroblast growth factors 15/19 and 21: from feast to famine. *Genes Dev.* **26,** 312–324
25. Badman, M. K., Pissios, P., Kennedy, A. R., Koukos, G., Flier, J. S., and Maratos-Flier, E. (2007) Hepatic fibroblast growth factor 21 is regulated by PPARα and is a key mediator of hepatic lipid metabolism in ketotic states. *Cell Metab.* **5,** 426–437
26. Inagaki, T., Dutchak, P., Zhao, G., Ding, X., Gautron, L., Parameswara, V., Li, Y., Goetz, R., Mohammadi, M., Esser, V., Elmquist, J. K., Gerard, R. D., Burgess, S. C., Hammer, R. E., Mangelsdorf, D. J., and Kliewer, S. A. (2007) Endocrine regulation of the fasting response by PPARα-mediated induction of fibroblast growth factor 21. *Cell Metab.* **5,** 415–425
27. Gälman, C., Lundåsen, T., Kharitonenkov, A., Bina, H. A., Eriksson, M., Hafström, I., Dahlin, M., Amark, P., Angelin, B., and Rudling, M. (2008) The circulating metabolic regulator FGF21 is induced by prolonged fasting and PPARα activation in man. *Cell Metab.* **8,** 169–174
28. Christodoulides, C., Dyson, P., Sprecher, D., Tsintzas, K., and Karpe, F. (2009) Circulating fibroblast growth factor 21 is induced by peroxisome proliferator-activated receptor agonists but not ketosis in man. *J. Clin. Endocrinol. Metab.* **94,** 3594–3601
29. Kharitonenkov, A., Shiyanova, T. L., Koester, A., Ford, A. M., Micanovic, R., Galbreath, E. J., Sandusky, G. E., Hammond, L. J., Moyers, J. S., Owens, R. A., Gromada, J., Brozinick, J. T., Hawkins, E. D., Wroblewski, V. J., Li, D. S., Mehrbod, F., Jaskunas, S. R., and Shanafelt, A. B. (2005) FGF-21 as a novel metabolic regulator. *J. Clin. Invest.* **115,** 1627–1635
30. Xu, J., Lloyd, D. J., Hale, C., Stanislaus, S., Chen, M., Sivits, G., Vonderfecht, S., Hecht, R., Li, Y. S., Lindberg, R. A., Chen, J. L., Jung, D. Y., Zhang, Z., Ko, H. J., Kim, J. K., and Véniant, M. M. (2009) Fibroblast growth factor 21 reverses hepatic steatosis, increases energy expenditure, and improves insulin sensitivity in diet-induced obese mice. *Diabetes* **58,** 250–259
31. Xu, J., Stanislaus, S., Chinookoswong, N., Lau, Y. Y., Hager, T., Patel, J., Ge, H., Weiszmann, J., Lu, S. C., Graham, M., Busby, J., Hecht, R., Li, Y. S., Li, Y., Lindberg, R., and Véniant, M. M. (2009) Acute glucose-lowering and insulin-sensitizing action of FGF21 in insulin-resistant mouse models–association with liver and adipose tissue effects. *Am. J. Physiol. Endocrinol. Metab.* **297,** E1105–E1114
32. Coskun, T., Bina, H. A., Schneider, M. A., Dunbar, J. D., Hu, C. C., Chen, Y., Moller, D. E., and Kharitonenkov, A. (2008) Fibroblast growth factor 21 corrects obesity in mice. *Endocrinology* **149,** 6018–6027
33. Fisher, F. M., Chui, P. C., Antonellis, P. J., Bina, H. A., Kharitonenkov, A., Flier, J. S., and Maratos-Flier, E. (2010) Obesity is a fibroblast growth factor 21 (FGF21)-resistant state. *Diabetes* **59,** 2781–2789
34. Zhang, X., Yeung, D. C., Karpisek, M., Stejskal, D., Zhou, Z. G., Liu, F., Wong, R. L., Chow, W. S., Tso, A. W., Lam, K. S., and Xu, A. (2008) Serum FGF21 levels are increased in obesity and are independently associated with the metabolic syndrome in humans. *Diabetes* **57,** 1246–1253
35. Li, H., Bao, Y., Xu, A., Pan, X., Lu, J., Wu, H., Lu, H., Xiang, K., and Jia, W. (2009) Serum fibroblast growth factor 21 is associated with adverse lipid profiles and γ-glutamyltransferase but not insulin sensitivity in Chinese subjects. *J. Clin. Endocrinol. Metab.* **94,** 2151–2156
36. Chavez, A. O., Molina-Carrion, M., Abdul-Ghani, M. A., Folli, F., Defronzo, R. A., and Tripathy, D. (2009) Circulating fibroblast growth factor-21 is elevated in impaired glucose tolerance and type 2 diabetes and

correlates with muscle and hepatic insulin resistance. *Diabetes Care* **32,** 1542–1546
37. Li, H., Fang, Q., Gao, F., Fan, J., Zhou, J., Wang, X., Zhang, H., Pan, X., Bao, Y., Xiang, K., Xu, A., and Jia, W. (2010) Fibroblast growth factor 21 levels are increased in nonalcoholic fatty liver disease patients and are correlated with hepatic triglyceride. *J. Hepatol.* **53,** 934–940
38. Li, H., Dong, K., Fang, Q., Hou, X., Zhou, M., Bao, Y., Xiang, K., Xu, A., and Jia, W. (2013) High serum level of fibroblast growth factor 21 is an independent predictor of non-alcoholic fatty liver disease: a 3-year prospective study in China. *J. Hepatol.* **58,** 557–563
39. Yan, H., Xia, M., Chang, X., Xu, Q., Bian, H., Zeng, M., Rao, S., Yao, X., Tu, Y., Jia, W., and Gao, X. (2011) Circulating fibroblast growth factor 21 levels are closely associated with hepatic fat content: a cross-sectional study. *PLoS One* **6,** e24895
40. Giannini, C., Feldstein, A. E., Santoro, N., Kim, G., Kursawe, R., Pierpont, B., and Caprio, S. (2013) Circulating levels of FGF-21 in obese youth: associations with liver fat content and markers of liver damage. *J. Clin. Endocrinol. Metab.* **98,** 2993–3000
41. De Sousa-Coelho, A. L., Marrero, P. F., and Haro, D. (2012) Activating transcription factor 4-dependent induction of FGF21 during amino acid deprivation. *Biochem. J.* **443,** 165–171
42. Schaap, F. G., Kremer, A. E., Lamers, W. H., Jansen, P. L., and Gaemers, I. C. (2013) Fibroblast growth factor 21 is induced by endoplasmic reticulum stress. *Biochimie* **95,** 692–699
43. Kim, K. H., Jeong, Y. T., Oh, H., Kim, S. H., Cho, J. M., Kim, Y. N., Kim, S. S., Kim do, H., Hur, K. Y., Kim, H. K., Ko, T., Han, J., Kim, H. L., Kim, J., Back, S. H., Komatsu, M., Chen, H., Chan, D. C., Konishi, M., Itoh, N., Choi, C. S., and Lee, M. S. (2013) Autophagy deficiency leads to protection from obesity and insulin resistance by inducing Fgf21 as a mitokine. *Nat. Med.* **19,** 83–92
44. Shao, M., Shan, B., Liu, Y., Deng, Y., Yan, C., Wu, Y., Mao, T., Qiu, Y., Zhou, Y., Jiang, S., Jia, W., Li, J., Li, J., Rui, L., and Yang, L. (2014) Hepatic IRE1α regulates fasting-induced metabolic adaptive programs through the XBP1s-PPARα axis signalling. *Nat. Commun.* **5,** 3528
45. Chitturi, S., Farrell, G. C., Hashimoto, E., Saibara, T., Lau, G. K., and Sollano, J. D. (2007) Non-alcoholic fatty liver disease in the Asia-Pacific region: definitions and overview of proposed guidelines. *J. Gastroenterol. Hepatol.* **22,** 778–787
46. Kleiner, D. E., Brunt, E. M., Van Natta, M., Behling, C., Contos, M. J., Cummings, O. W., Ferrell, L. D., Liu, Y. C., Torbenson, M. S., Unalp-Arida, A., Yeh, M., McCullough, A. J., and Sanyal, A. J. (2005) Design and validation of a histological scoring system for nonalcoholic fatty liver disease. *Hepatology* **41,** 1313–1321
47. Mao, T., Shao, M., Qiu, Y., Huang, J., Zhang, Y., Song, B., Wang, Q., Jiang, L., Liu, Y., Han, J. D., Cao, P., Li, J., Gao, X., Rui, L., Qi, L., and Li, W. (2011) PKA phosphorylation couples hepatic inositol-requiring enzyme 1α to glucagon signaling in glucose metabolism. *Proc. Natl. Acad. Sci. U.S.A.* **108,** 15852–15857
48. Wang, Q., Jiang, L., Wang, J., Li, S., Yu, Y., You, J., Zeng, R., Gao, X., Rui, L., Li, W., and Liu, Y. (2009) Abrogation of hepatic ATP-citrate lyase protects against fatty liver and ameliorates hyperglycemia in leptin receptor-deficient mice. *Hepatology* **49,** 1166–1175
49. Kurosu, H., Choi, M., Ogawa, Y., Dickson, A. S., Goetz, R., Eliseenkova, A. V., Mohammadi, M., Rosenblatt, K. P., Kliewer, S. A., and Kuro-o, M. (2007) Tissue-specific expression of βKlotho and fibroblast growth factor (FGF) receptor isoforms determines metabolic activity of FGF19 and FGF21. *J. Biol. Chem.* **282,** 26687–26695
50. Zhang, X., Ibrahimi, O. A., Olsen, S. K., Umemori, H., Mohammadi, M., and Ornitz, D. M. (2006) Receptor specificity of the fibroblast growth factor family. The complete mammalian FGF family. *J. Biol. Chem.* **281,** 15694–15700
51. Ogawa, Y., Kurosu, H., Yamamoto, M., Nandi, A., Rosenblatt, K. P., Goetz, R., Eliseenkova, A. V., Mohammadi, M., and Kuro-o, M. (2007) βKlotho is required for metabolic activity of fibroblast growth factor 21. *Proc. Natl. Acad. Sci. U.S.A.* **104,** 7432–7437
52. Yamamoto, K., Yoshida, H., Kokame, K., Kaufman, R. J., and Mori, K. (2004) Differential contributions of ATF6 and XBP1 to the activation of endoplasmic reticulum stress-responsive cis-acting elements ERSE, UPRE and ERSE-II. *J. Biochem.* **136,** 343–350
53. Yamamoto, K., Takahara, K., Oyadomari, S., Okada, T., Sato, T., Harada, A., and Mori, K. (2010) Induction of liver steatosis and lipid droplet formation in ATF6α-knockout mice burdened with pharmacological endoplasmic reticulum stress. *Mol. Biol. Cell* **21,** 2975–2986
54. Lee, A. H., Scapa, E. F., Cohen, D. E., and Glimcher, L. H. (2008) Regulation of hepatic lipogenesis by the transcription factor XBP1. *Science* **320,** 1492–1496
55. Li, B., Pi, Z., Liu, L., Zhang, B., Huang, X., Hu, P., Chevet, E., Yi, P., and Liu, J. (2013) FGF-2 prevents cancer cells from ER stress-mediated apoptosis via enhancing proteasome-mediated Nck degradation. *Biochem. J.* **452,** 139–145
56. Dutchak, P. A., Katafuchi, T., Bookout, A. L., Choi, J. H., Yu, R. T., Mangelsdorf, D. J., and Kliewer, S. A. (2012) Fibroblast growth factor-21 regulates PPARγ activity and the antidiabetic actions of thiazolidinediones. *Cell* **148,** 556–567
57. Lin, Z., Tian, H., Lam, K. S., Lin, S., Hoo, R. C., Konishi, M., Itoh, N., Wang, Y., Bornstein, S. R., Xu, A., and Li, X. (2013) Adiponectin mediates the metabolic effects of FGF21 on glucose homeostasis and insulin sensitivity in mice. *Cell Metab.* **17,** 779–789
58. Holland, W. L., Adams, A. C., Brozinick, J. T., Bui, H. H., Miyauchi, Y., Kusminski, C. M., Bauer, S. M., Wade, M., Singhal, E., Cheng, C. C., Volk, K., Kuo, M. S., Gordillo, R., Kharitonenkov, A., and Scherer, P. E. (2013) An FGF21-adiponectin-ceramide axis controls energy expenditure and insulin action in mice. *Cell Metab.* **17,** 790–797